Nanoscale Res Lett (2010) 5:1128–1131
DOI 10.1007/s11671-010-9613-2

NANO EXPRESS

Field Emission of ITO-Coated Vertically Aligned Nanowire Array

Chang Hwa Lee · Seok Woo Lee · Seung S. Lee

Received: 25 January 2010 / Accepted: 13 April 2010 / Published online: 29 April 2010

Abstract An indium tin oxide (ITO)-coated vertically aligned nanowire array is fabricated, and the field emission characteristics of the nanowire array are investigated. An array of vertically aligned nanowires is considered an ideal structure for a field emitter because of its parallel orientation to the applied electric field. In this letter, a vertically aligned nanowire array is fabricated by modified conventional UV lithography and coated with 0.1-μm-thick ITO. The turn-on electric field intensity is about 2.0 V/μm, and the field enhancement factor, β, is approximately 3,078 when the gap for field emission is 0.6 μm, as measured with a nanomanipulator in a scanning electron microscope.

Keywords Field emission · ITO · Nanowire · Top–down

Field emission is quantum mechanical tunneling of electrons through the surface potential barrier into vacuum [1], which has been widely exploited in vacuum electronic applications including electron guns, microwave tubes, and flat panel displays [2]. Vertically aligned nanowire array (VANA) shows excellent field emission properties owing to a strong local electric field due to their parallel orientation to the applied electric field [3]. Numerous studies have been carried out on the fabrication of VANAs as field emitters using bottom-up synthesis approaches [4–6]. However, these bottom-up methods have drawbacks such as an expensive process and relatively low fabrication reliability, thus making them unsuitable for mass production.

In this letter, a top–down method of modified conventional UV lithography is suggested for the fabrication of a VANA, thereby resolving the problems of bottom-up methods while allowing control over the VANA's position and shape. In the lithography process, a photoresist VANA is fabricated with a UV exposure dose control. After the lithography, a carbonization process (pyrolysis process) is followed to provide volume contraction of the array's structure. The pyrolyzed carbon VANA is coated with a 0.1-μm-thick ITO layer in order to realize a durable field emitter and to provide low turn-on voltage [7, 8]. ITO has good transparence characteristics in the visible region of the electromagnetic spectrum while maintaining high electrical conductivity, thermal stability, and oxidation resistance [4, 9]. In a field emission experiment, a nanomanipulator in a scanning electron microscope (SEM) is used in order to measure field emission while precisely controlling the distance between the anode and cathode (field emitter).

The fabrication process of the ITO-coated VANA is shown in Fig. 1. Figure 1a shows circular aperture patterns ($\varphi = 1$ μm) of a 0.1-μm-thick chrome (Cr) layer on a fused silica wafer. SU-8 50 (Microchem Co.) is deposited on the Cr layer in Fig. 1b. The backside of the fused silica wafer is exposed to UV light filtered by a narrow band-pass filter ($\lambda = 365$ nm and bandwidth = 10 nm, OptoSigma Co.) with an exposure dose of 200 mJ/cm^2 in Fig. 1c. The intensity of UV light is concentrated to the central axis by diffraction in the SU-8 medium, which defines a sharp, high aspect ratio SU-8 structure [10]. After development of SU-8 and Cr etching, the SU-8 VANA is obtained, as shown in Fig. 1d. Figure 1e shows the pyrolyzed carbon VANA obtained by a pyrolysis process in a quartz tube

C. H. Lee · S. W. Lee (✉) · S. S. Lee
Department of Mechanical Engineering, Korea Advanced Institute of Science and Technology, Daejeon 305-701, Korea
e-mail: swlee81@kaist.ac.kr

furnace at 900°C for 30 min [11]. Volume shrinkage to approximately 60% occurs in this process for the SU-8 VANA. Finally, Fig. 1f shows the VANA coated with a 0.1-µm-thick ITO layer. The size of VANA is controlled by the circular aperture patterns of a Cr layer on a fused silica wafer and the aspect ratio by the UV light exposure dose.

Figures 2a–c are the fabrication results of Fig. 1d–f, respectively. Figure 2a shows a SEM image of a SU-8 VANA with a diameter of 1 µm produced with an UV exposure dose of 200 mJ/cm^2. The aspect ratio of the structure is more than 7. Figure 2b shows the pyrolyzed carbon VANA after pyrolysis, where the volume shrinkage is 60% and the aspect ratio is increased to more than 9. Figure 2c shows the ITO-coated VANA with 0.1-µm-thick ITO layer. Utsumi concluded that the best field emitter should be high aspect ratio rounded whisker like this ITO-coated VANA [12]. Figure 2d presents energy dispersive spectrum (EDS) results showing the chemical composition of the ITO-coated VANA, which comprises In, Sn, O, C, and Si.

Figure 3a presents a schematic view of the experimental setup for investigating the field emission characteristics with a Zyvex nanomanipulator (Zyvex Instrument) operating inside a SEM vacuum chamber. The nanomanipulator controls the distance between the ITO-coated VANA, the field emitter, and the tungsten tip A, the counter electrode. The tungsten tip A, the anode, is connected to the (+) of a Keithley 4200 (Keithley Instrument Inc.), while the tungsten tip B, the cathode, on the surface of the wafer is connected to the (-) of the instrument via a feed through to apply voltage and to sense current. Figure 3b shows a SEM image of the ITO VANA and the tungsten tip A in a SEM vacuum chamber of 1.59×10^{-5}torr.

With the shortest distance, d, of 0.6 µm, the current is measured by the Keithley 4200 using the voltage sweep function. As the voltage and the distance are known, the I-E curve of the ITO-coated VANA can be determined, as shown in Fig. 4a. As the electric field intensity (E) is increased, the current (I) increases exponentially, following the behavior of the Fowler–Nordheim (F–N) equation. The field emission starts around 2.0 V/µm and the maximum current is 4.0×10^{-6} A. Figure 4b shows the F–N curve obtained from the I-E curve of the ITO-coated VANA. This curve shows a linear relationship after turn-on electric field intensity, following the F–N equation, as indicated by the red line. The turn-on electric field intensity is 2.0/µm, which can be estimated where the slope of the F–N curve changes. Figure 4c shows the field emission current stability of the ITO-coated VANA over a period of 3 min, measured under a vacuum of 1.59×10^{-5}torr when the electric field intensity (E) is 2.5 V/µm.

In order to estimate the field enhancement factor, β, F–N parameters are evaluated by linear fit of the red line in Fig. 4b. The field emission is described by the F–N equation as follows [1, 13],

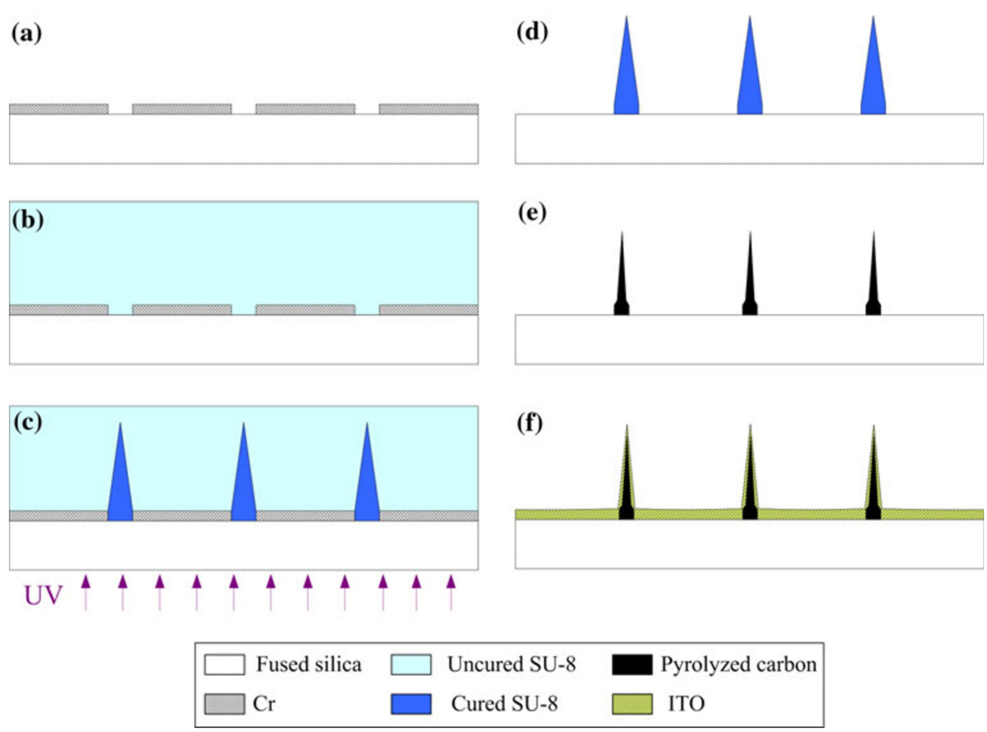

Fig. 1 Schematic view of fabrication process of ITO-coated VANA. **a** Circular aperture patterns ($\varphi = 1$ µm) of Cr layer on a fused silica wafer. **b** SU-8 50 on Cr layer. **c** Backside UV exposure with exposure dose of 200 mJ/cm^2 filtered by a narrow band-pass filter. **d** SU-8 VANA after development of SU-8 and Cr etching. **e** Pyrolyzed carbon VANA by pyrolysis process at 900°C for 30 min. **f** ITO-coated VANA with 0.1-µm-thick ITO

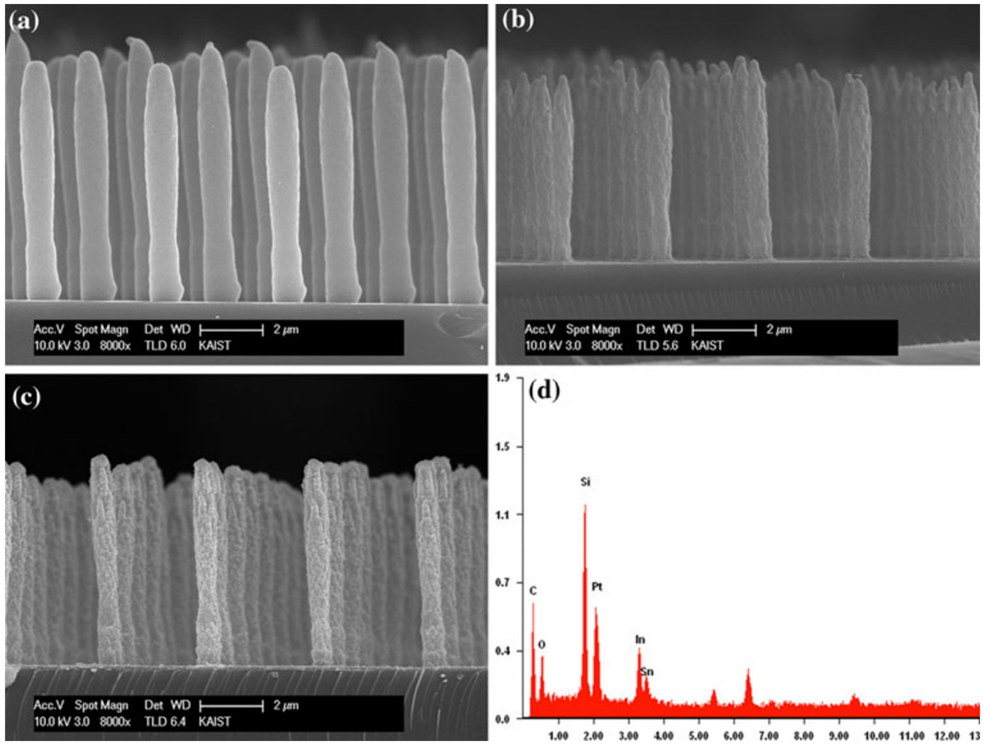

Fig. 2 SEM images of **a** SU-8 VANA, **b** pyrolyzed carbon VANA, and **c** ITO-coated VANA. **d** EDS result of ITO-coated VANA

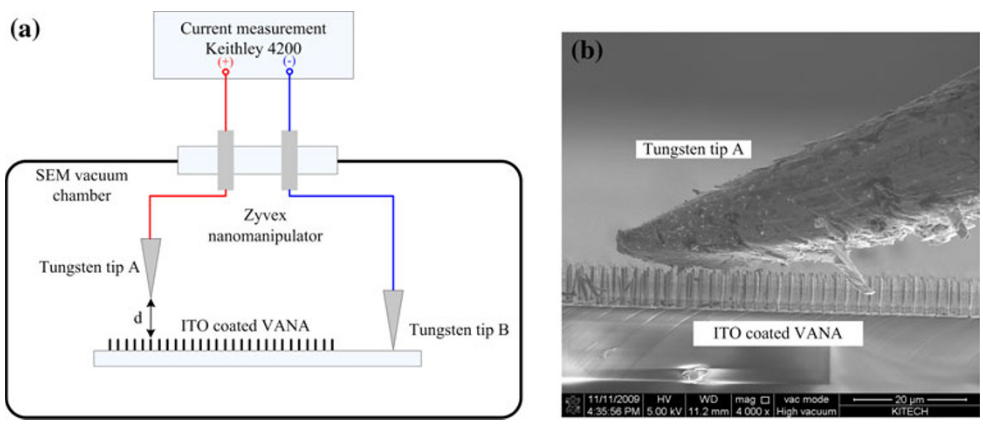

Fig. 3 **a** Schematic view of the experimental setup, where a Zyvex nanomanipulator is employed in a SEM vacuum chamber. **b** SEM image of the tungsten tip A and ITO-coated VANA with distance control by the nanomanipulator

$$I(E) = A\frac{q}{8\phi^2\hbar}\frac{1}{\varphi}(\beta E)^2 \exp\left(-\frac{4}{3\hbar(\beta E)}\sqrt{2m\varphi^3}\right) \quad (1)$$

where I, E, β, φ, A, $\hbar$, and m are the current, electric field intensity, field enhancement factor, work function, area, reduced Planck constant, and electron mass, respectively. This equation explains the shape of the I-E curve in Fig. 4a and can be modified as follows,

$$\left(\ln\frac{I}{E^2}\right) = -\frac{b}{\beta}\varphi^{\frac{3}{2}}\left(\frac{1}{E}\right) + \ln aA\beta^2 = -21.18\left(\frac{1}{E}\right) - 5.76$$
$$\left(b = 6.83\times 10^3 V^{-\frac{1}{2}}\mu m^{-1}\right) \quad (2)$$

Note that −21.18 is the slope of the red line and −5.76 is the y-intercept of the red line in Fig. 4b. The estimated field enhancement factor of the ITO-coated VANA, β, is 3,078 when the work function of ITO is 4.5 eV [9]. The measured value of the field enhancement factor is comparable with previous research results of field emitters [4, 14, 15].

In summary, an ITO-coated VANA was fabricated by a top–down method using modified conventional UV lithography, and the field emission characteristics were evaluated using a Zyvex nanomanipulator. The top–down method offers many advantages including an economical process, good fabrication reliability, and suitability for mass production. The turn-on electric field intensity of the ITO-coated VANA is about 2.0 V/µm, and the estimated field enhancement factor β is 3,078. These results show

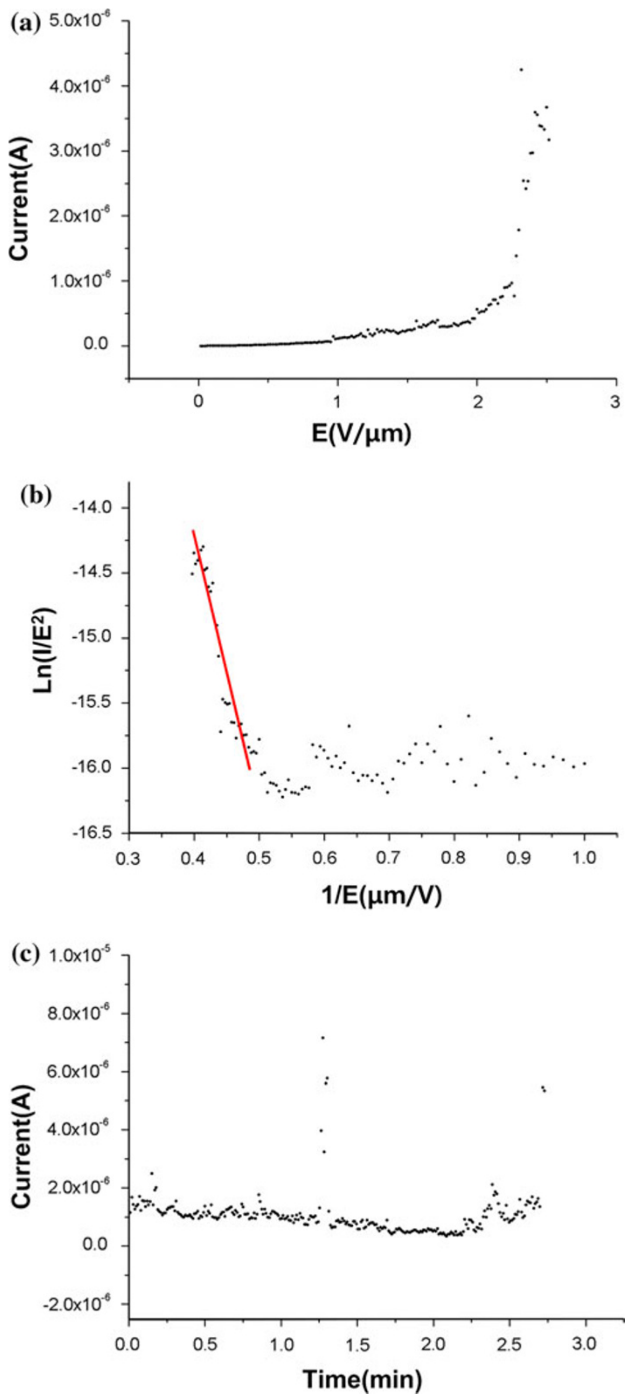

Fig. 4 a Field emission I-E curve of the ITO-coated VANA measured under a vacuum of 1.59×10^{-5} torr. **b** Corresponding F–N curve obtained from I-E curve. **c** Field emission current stability of ITO-coated VANA at 1.59×10^{-5} torr

that the ITO-coated VANA is a very promising candidate for vacuum electron field emission applications.

Acknowledgments This work was partly supported by Brain Korea 21 and Award No KUK-F1-038-02, made by King Abdullah University of Science and Technology (KAUST).

References

1. R.H. Fowler, L. Nordheim, Proc. R. Soc. Lond. **A119**, 173 (1928)
2. I. Brodie, P.R. Schwoebel, Proc. IEEE **82**, 1006–1034 (1994)
3. W.I. Milne, K.B.K. Teo, G.A.J. Amaratunga, R. Lacerda, P. Legagneux, G. Pirio, V. Semet, V. Thien Binh, Curr. Appl. Phys. **4**, 513–551 (2004)
4. Q. Wan, P. Feng, T.H. Wang, Appl. Phys. Lett. **89**, 123102 (2006)
5. A.V. Melechko, V.I. Merkulov, T.E. McKnight, M.A. Guillorn, K.L. Klein, D.H. Lowndes, M.L. Simpson, J. Appl. Phys. **97**, 041301 (2005)
6. C.J. Lee, T.J. Lee, S.C. Lyu, Y. Zhang, H. Ruh, H.J. Lee, Appl. Phys. Lett. **81**, 3648 (2002)
7. R.S. Chen, Y.S. Huang, Y.M. Liang, C.S. Hsieh, D.S. Tsai, K.K. Tiong, Appl. Phys. Lett. **84**, 1552 (2004)
8. M. Ollinger, V. Craciun, R.K. Singh, Appl. Phys. Lett. **80**, 1927 (2004)
9. Y. Park, V. Choong, Y. Gao, B.R. Hsieh, C.W. Tang, Appl. Phys. Lett. **68**, 2699 (1996)
10. S.W. Lee, S.S. Lee, Opt. Lett. **33**, 40 (2008)
11. J.A. Lee, S.W. Lee, K.-C. Lee, S.I. Park, S.S. Lee, J. Micromech. Microeng. **18**, 035012 (2008)
12. T. Utsumi, IEEE Trans. Electron Dev. **38**, 2276 (1991)
13. X. Lu, Q. Yang, C. Xiao, A. Hirose, T. Tiedje, J. Phys. D Appl. Phys. **40**, 4010 (2007)
14. L. Nilsson, O. Groening, C. Emmenegger, O. Kuettel, E. Schaller, L. Schlapbach, H. Kind, J.-M. Bonard, K. Kern, Appl. Phys. Lett. **76**, 2071 (2000)
15. H. Jia, Y. Zhang, X. Chen, J. Shu, X. Luo, Z. Zhang, D. Yu, Appl. Phys. Lett. **82**, 4146 (2003)